Modeling Cytoskeletal Traffic: An Interplay between Passive Diffusion and Active Transport

Izaak Neri,[1,2] Norbert Kern,[1,2] and Andrea Parmeggiani[1,2,3,4]

[1]*Laboratoire Charles Coulomb UMR 5221, Université Montpellier 2, F-34095 Montpellier, France*
[2]*Laboratoire Charles Coulomb UMR 5221, CNRS, F-34095 Montpellier, France*
[3]*Laboratoire DIMNP UMR 5235, Université Montpellier 2, F-34095 Montpellier, France*
[4]*Laboratoire DIMNP UMR 5235, CNRS, F-34095 Montpellier, France*

(Received 6 September 2012; published 28 February 2013)

We introduce the totally asymmetric simple exclusion process with Langmuir kinetics on a network as a microscopic model for active motor protein transport on the cytoskeleton, immersed in the diffusive cytoplasm. We discuss how the interplay between active transport along a network and infinite diffusion in a bulk reservoir leads to a heterogeneous matter distribution on various scales: we find three regimes for steady state transport, corresponding to the scale of the network, of individual segments, or local to sites. At low exchange rates strong density heterogeneities develop between different segments in the network. In this regime one has to consider the topological complexity of the whole network to describe transport. In contrast, at moderate exchange rates the transport through the network decouples, and the physics is determined by single segments and the local topology. At last, for very high exchange rates the homogeneous Langmuir process dominates the stationary state. We introduce effective rate diagrams for the network to identify these different regimes. Based on this method we develop an intuitive but generic picture of how the stationary state of excluded volume processes on complex networks can be understood in terms of the single-segment phase diagram.

DOI: 10.1103/PhysRevLett.110.098102 PACS numbers: 87.16.A−, 05.60.Cd, 87.16.Uv, 89.75.Hc

Introduction.—Statistical physics has been very successful in deducing macroscopic properties of materials from the interactions between their microscopic components. Active matter systems, on the other hand, such as active colloids, animal flocks, or cytoskeletal assemblies, are prone to develop out-of-equilibrium patterns. These spatial heterogeneities are in fact essential to life processes [1].

Here we would like to initiate a microscopic statistical physics approach to describe the collective organization of molecular motors in cells. Motor proteins navigate actively throughout the cell [2,3] along the cytoskeleton, a network of filamentous assemblies spanning the cytoplasm. These proteins can exert forces, depolymerize filaments and transport biological cargos along the cytoskeleton [4], and thus play an important role in the assembly, self-organization, and functioning of cells [5]. Single-molecule properties of the motors are well studied and can now be measured accurately *in vivo* [6]. But understanding how motors collectively self-organize remains a very important step in developing a microscopic vision of intracellular organization.

Macroscopic approaches to study intracellular motor protein transport have been developed [7], including efforts to introduce microscopic aspects [8,9], but a generic microscopic picture of cytoskeletal transport has yet to emerge. Here we present a tentative approach using a minimalistic model for cytoskeletal active transport, which consists of directed motion of particles (motor proteins) along the network (cytoskeleton) and diffusion in the bulk (cytoplasm), see Fig. 1. We model the directed motion along the cytoskeleton using the totally asymmetric simple exclusion process (TASEP) [10] along a disordered directed network [11]. The binding and unbinding of particles between the network and the bulk is represented via Langmuir kinetics (LK) [12]. We consider the particles in the bulk to be infinitely diffusive which, as we will show, is a relevant limiting case.

TASEP is a fundamental model in nonequilibrium physics [13], but it is also used in more applied topics, such as modeling macromolecules moving through capillary vessels [14], electrons hopping through a quantum-dot chain [15], and vehicular traffic [16]. LK, on the other hand, is a well-known fundamental equilibrium process in chemical physics [12].

Our model constitutes a generalization of transport through closed networks [11] to open systems, as they

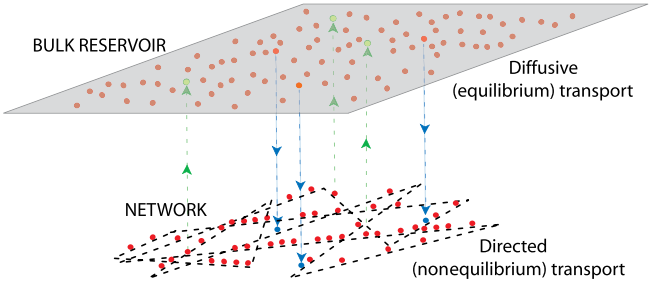

FIG. 1 (color online). Statistical physics model of cytoskeletal transport, capturing the competition between active transport of particles through a network (cytoskeleton) with diffusion in a bulk reservoir (cytoplasm).

 © 2013 American Physical Society

are relevant for cytoskeletal transport. It may also be seen as a generalization to a large scale network of the totally asymmetric exclusion process with Langmuir kinetics (TASEP-LK) on a single segment [17], which has been shown to quantitatively describe *in vitro* experiments of motor proteins [18]. Our study differs from previous work [8] in that we consider exclusion interactions and disordered networks, both essential points to the physical picture we develop.

The fundamental question we address is how spatial heterogeneities emerge in such open active systems, here due to the competition between diffusion in a reservoir (which spreads particles homogeneously) and active transport along a network (which generates heterogeneities [11]). We will show how this competition is governed by the hopping rate for particles on the network, the exchange rates with the reservoir, and the filament length. One main result of our work is that there exist three regimes of transport through complex networks which are linked to the scale at which spatial density heterogeneities arise: the *network*, the *segments*, or the *sites*.

Microscopic model for cytoskeletal transport.—We represent the cytoskeleton as a network of directed segments of L sites each, connected by junction sites, see Fig. 2(a). We use random networks to reflect the topological complexity of the cytoskeleton, a standard approach in modeling networks [19]. Specifically we use Erdös-Rényi graphs of mean connectivity c, as in Ref. [11]. Whereas the specific topology is not important for our qualitative results, the fact that networks are *irregular*, i.e., that the number of incoming c_v^{i} and outgoing c_v^{o} segments of the junction v differ, is relevant.

In each directed segment particles move according to TASEP-LK rules [17]: particles hop unidirectionally at rate p, subject to exclusion interactions. Furthermore, particles obey binding-unbinding kinetics with attachment rate ω_A and detachment rate ω_D respectively, at every site along the network. Particles in the reservoir are assumed to diffuse infinitely fast.

The phase diagram of TASEP-LK has been determined [17] for a single segment connecting a reservoir with entry rate α to a reservoir with exit rate β (see Supplemental Material [20]). TASEP-LK is best characterized in terms

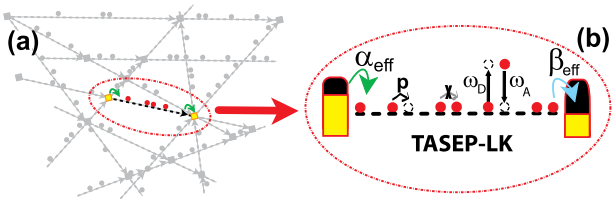

FIG. 2 (color online). Sketch of the method to study transport through complex networks here for TASEP-LK. Each segment of the network (a) is considered to connect to two reservoirs with effective rates α_{eff} and β_{eff} (b), which are set by the junction densities.

of the dimensionless parameters $\Omega_A = \omega_A L/p$ and $\Omega_D = \omega_D L/p$, where Ω_D quantifies the fraction of the segment which an isolated particle typically covers before detaching [17]. It is convenient to consider the parameters $\Omega = (\Omega_A + \Omega_D)/2$, characterizing the total exchange between reservoir and segment, and the ratio $K = \Omega_A/\Omega_D$, which sets the equilibrium Langmuir density $\rho_\ell = K/(K+1)$.

The (α, β)-phase diagram of TASEP-LK is fully characterized in terms of the parameters Ω and K (see Refs. [17,20] and Fig. 4). In the following, we refer to low density (LD), high density (HD) and maximum current (MC, or M for "Meissner" in Ref. [17]) phases. All of these reduce to TASEP phases with a flat density profile for $\Omega = 0$ [10]. Furthermore, LD and HD zones can coexist on the same segment separated by a domain wall, leading to a coexistence phase (LD-HD).

Mean field method for TASEP-LK on networks.—We analyze TASEP-LK by extending the mean field arguments for TASEP presented in Ref. [11]. In this approach every segment (v, v') connecting two vertices v and v' is considered to be governed by effective entry and exit rates $\alpha^{\mathrm{eff}}_{(v,v')}$ and $\beta^{\mathrm{eff}}_{(v,v')}$, see Fig. 2(c). These rates are in turn determined by the average densities ρ_v and $\rho_{v'}$ at the junction sites [11,21]: $\alpha^{\mathrm{eff}}_{v,v'} = p\rho_v/c^{\mathrm{o}}_v$ and $\beta^{\mathrm{eff}}_{v,v'} = p(1-\rho_{v'})$, where the latter condition reflects the exclusion constraint at the junctions. Balancing the currents at the junctions leads to the following closed set of equations in ρ_v:

$$\frac{\partial \rho_v}{\partial t} = \sum_{v' \to v} J^-\left[\frac{\rho_{v'}}{c^{\mathrm{o}}_{v'}}, 1-\rho_v\right] - \sum_{v' \leftarrow v} J^+\left[\frac{\rho_v}{c^{\mathrm{o}}_v}, 1-\rho_{v'}\right], \tag{1}$$

where the sums are over incoming (outgoing) segments, and $J^{\pm}[\alpha/p, \beta/p]$ are the currents entering (leaving) a segment with rates α (β). The expressions for $J^{\pm}$ are readily available [17,20]. Because of the Langmuir process, the current is not constant along the segment, such that $J^- \neq J^+$. Solving Eq. (1) yields the complete stationary state of all segments in the network.

The *overall* particle density on a network immersed in a reservoir is equal to the Langmuir density ρ_ℓ, set by the ratio K [22]. In the following we discuss the physical phenomena on the network at fixed K as the exchange parameter Ω interpolates from TASEP with purely active transport ($\Omega = 0$) to the limit at very high binding-unbinding rates where the passive diffusion process dominates ($\Omega \to \infty$). The data shown here have been obtained using $K = 1.5$, which is a reasonable value for motor proteins [23] and theoretically not specific in any way: our analysis is general, and only very high and very low values of K require an additional discussion [22].

Decoupling due to particle exchange.—In principle, the continuity equations (1) couple the densities ρ_v and $\rho_{v'}$ of those junctions which are linked by a segment (v, v'): it is this coupling which makes the transport problem global,

making it necessary to analyze the whole network simultaneously.

Here we exploit one feature of TASEP-LK, which we state by saying that the binding-unbinding process can "decouple" the currents at the segment boundaries. Indeed, for the composite LD-HD phase it is known [17] that the in-current J^- depends on the in-rate $\alpha^{\rm eff}$ only, whereas the out-current J^+ depends on the out-rate $\beta^{\rm eff}$ only. Any LD-HD segment therefore lifts one coupling constraint in Eq. (1), since the in and out currents $J^\pm$ are determined *locally* by the junction densities ρ_v and the local connectivity.

When complete decoupling is achieved, as is expected at high values of Ω, one can directly deduce the junction densities for an arbitrary network. As presented in the Supplemental Material [20], this leads to an exact solution of the mean field Eq. (1). For $K > 1$ we have

$$\rho_v = \begin{cases} c_v^{\rm o}\left(\frac{c_v^{\rm i}-1}{c_v^{\rm o}c_v^{\rm i}-1}\right), & \rho_v \le \frac{c_v^{\rm o}}{K+1}; c_v^{\rm i} \neq 1 \\ \frac{c_v^{\rm o}}{2}\left(1-\sqrt{1-\frac{c_v^{\rm i}}{c_v^{\rm o}}}\right), & \rho_v \le \frac{c_v^{\rm o}}{K+1}; c_v^{\rm i} = 1 \\ \frac{1}{2}+\sqrt{\frac{1}{4}-\frac{c_v^{\rm o}}{c_v^{\rm i}}\rho_\ell(1-\rho_\ell)}, & \rho_v \ge \frac{c_v^{\rm o}}{K+1}; \rho_v \ge \frac{1}{2}. \end{cases} \quad (2)$$

In Fig. 3 we compare these analytical predictions based on complete decoupling to both a (numerical) full mean-field solution to Eq. (1) and to simulations. For low values of Ω the fully coupled description in Eq. (1) is necessary (especially for low mean connectivity c). Surprisingly, the decoupled description in Eq. (2) is excellent even down to relatively low values of Ω. This is an important result, as it shows that single segment TASEP-LK [17] suffices to describe transport through any complex network for a wide Ω range. For comparison, we have also indicated the average mean-field current in the $c \to \infty$ limit, i.e., the TASEP-LK current which is maintained even when all junctions are blocked ($\alpha^{\rm eff} = \beta^{\rm eff} = 0$). This constitutes a lower bound to any current in any network.

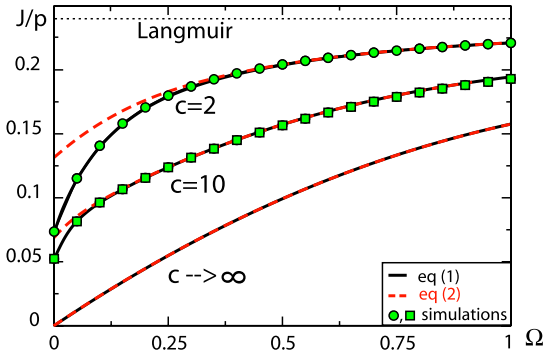

FIG. 3 (color online). Average current as a function of the exchange parameter Ω, for three different (average) connectivities ($c = 2$, $c = 10$, and $c \to \infty$) at $K = 1.5$. Agreement between simulation (symbols, for $L = 400$) and mean-field results [solid lines, Eq. (1)] is excellent. The (red) dashed line is the current obtained from the simplified mean-field result [Eq. (2)] while the dotted line denotes the Langmuir current $J/p = \rho_\ell(1-\rho_\ell)$. Results are for a single graph instance of $O(10^2)$ junctions.

Effective rate plots.—Here we introduce effective rate plots as a way to understand intuitively the physics of active transport through networks by allowing visualization of the whole stationary transport state of the network. In Fig. 4 we map the effective rates (α_s, β_s) of each segment s, obtained by numerically solving the full mean field Eq. (1), onto the single segment phase diagram. Note that the scattering of effective rates is due to the irregularity of the networks considered.

For sufficiently high c Fig. 4 reveal that the effective rates cluster close to the origin, in the LD-HD phase; this explains why the simplified Eq. (2) work well for high c in Fig. 3. When increasing Ω the TASEP-LK phase diagram changes. In particular, the LD phase reduces in favor of the LD-HD phase. Moreover, at high Ω one notices a specific alignment of the effective rates as given by the decoupled Eq. (2).

In the following section we show how effective rate plots allow us to rationalize the scale at which density heterogeneities appear in the network.

Heterogeneities for TASEP-LK on irregular networks.—The parameter Ω regulates the way particles distribute along the network, at *overall* density ρ_ℓ, and thus determines how heterogeneities develop. We characterize the stationary state from the effective rate plots by determining the fraction of segments occupying the corresponding phases, see Fig. 5. A complementary point of view is given in Fig. 6 with the distribution $W(\rho_s)$ of the mean segment densities ρ_s in the network. From these figures we conclude that heterogeneities develop throughout the network

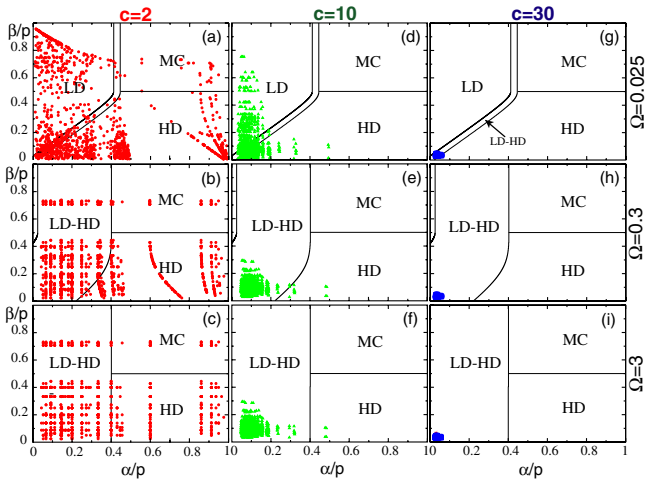

FIG. 4 (color online). Effective rate diagrams for irregular graphs of mean connectivity c (at $K = 1.5$, for given values of Ω). Effective rates follow from solving Eq. (1). Single graph instances consisted of $O(10^2)$ junctions.

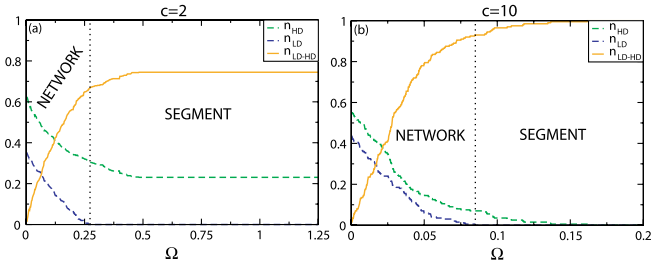

FIG. 5 (color online). Fraction of segments in LD, HD, and LD-HD phases, in the effective rate diagram of mean connectivity (a) $c = 2$ and (b) $c = 10$, for $K = 1.5$. The transition Ω_c between the network and the segment regime (denoted by the vertical dotted line) is determined by the condition that n_{LD} vanishes. The graph instances used are those of Fig. 4.

in three successive regimes (we discuss the case $K > 1$ and refer to Ref. [22] for $K \leq 1$): (i) The *network* regime, for low exchange rates Ω, is characterized by the presence of LD and HD segments. The distribution $W(\rho_s)$ is marked by the LD and HD peaks (whereas LD-HD coexistence segments are distributed evenly over the intermediate density range). This bimodality implies a strongly heterogeneous density at the network scale. (ii) In the *segment* regime, for intermediate exchange rates, all LD segments have disappeared in favor of LD-HD segments. The distribution $W(\rho_s)$ is dominated by the LD-HD peak. Although all segments have similar average densities, the presence of domain walls implies strong inhomogeneities on the segment scale. (iii) In the *Langmuir* regime, for large exchange rates Ω, the Langmuir phase dominates. All segments have homogeneous densities except for small regions near the boundaries, and no heterogeneities arise beyond the scale of a few *sites*.

The transition between the network and segment regimes is sharp (identified as the point Ω_c where all LD segments disappear, $n_{\mathrm{LD}} = 0$). Moreover, this transition has an upper bound $\Omega^* = 1/2 + f(K) \ln\{f(K)/[1/2 + f(K)]\}$ (with $f(K) = |K - 1|/[2(K + 1)]$), for which the LD phase disappears from the single segment phase diagram [22]. In contrast, the crossover from the segment regime to the Langmuir regime is progressive.

Conclusions.—We have analyzed active transport on a disordered network immersed in a bulk reservoir, as may be considered a simple model for cytoskeletal transport by motor proteins. The dimensionless parameter Ω characterizes the importance of particle exchange with the reservoir with respect to active transport on the network. Ω therefore also quantifies the competition between the heterogeneities on the network, where particles undergo active transport, and the homogenizing effect of the reservoir, where particles diffuse infinitely fast.

Three regimes arise, according to the scale at which heterogeneities appear in the network: a *network*, a *segment,* and a *Langmuir* (site-dominated) regime, see Fig. 7. Interestingly, these scales also set the complexity that characterizes the theoretical analysis. In the network regime, TASEP-LK transport is coupled throughout the network, whereas in the opposite Langmuir regime the physics is essentially determined by the attachment-detachment process. In the intermediate segment regime, decoupling implies that the transport characteristics of all segments follows from those of a single segment.

Effective rate plots allow us to intuitively understand transport processes through networks from the single-segment transport characteristics; from the scattering of rates over both the LD and HD zones we can directly deduce the role of strong heterogeneities, see Fig. 4. This approach yields valuable *a priori* insight into yet more complex excluded volume transport such as TASEP with extended particles [24], TASEP with multiple species [25], and, as we show in Ref. [22], bidirectional motion [26]. As in TASEP-LK, the single-segment phase diagram serves as a basis for deducing the behavior on the network. From the effective rate diagram approach it becomes also clear that our results extend to types of disorder other than topological which are relevant to biological systems, e.g., disorder

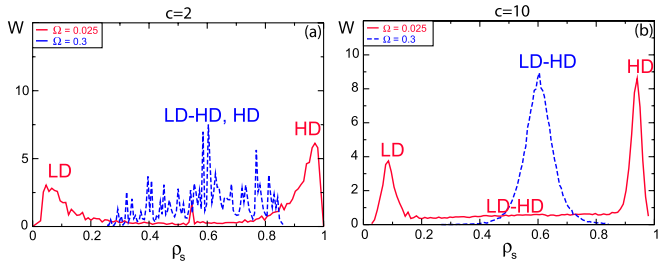

FIG. 6 (color online). The mean field distribution $W(\rho_s)$ of segment densities for an irregular graph instance with mean connectivity (a) $c = 2$ and (b) $c = 10$, of $O(10^4)$ junctions, for $K = 1.5$. At low values the bimodal distribution of Ref. [11] is identified. When increasing Ω the center peak gradually grows while the edge peaks shrink. Network heterogeneities eventually disappear at intermediate $\Omega = \Omega_c$, leading to a unimodal density distribution.

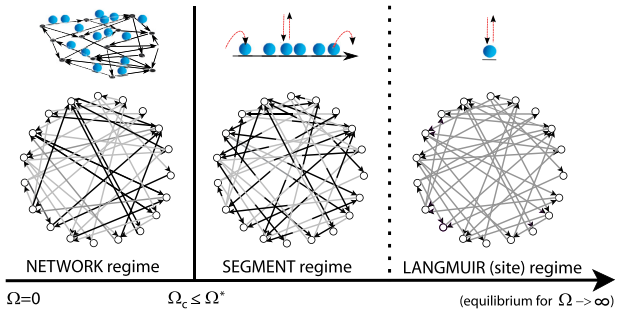

FIG. 7 (color online). Illustration of the three regimes with heterogeneities on a network, segment, and site scale, respectively, according to the exchange parameter Ω (see main text for Ω_c and Ω^*). Particle densities are coded in gray scale. Pictorials on top indicate the scale at which continuity equations are solved.

in the actions of particles at the junctions [21,27]. An interesting open question is how finite diffusion [28] could be handled within our approach.

Several conclusions may be relevant for modeling cytoskeletal transport. First, we have shown that strong inhomogeneities in the spatial distribution of motor proteins form for a wide range of parameters. Even in the case of infinitely fast diffusion considered here they resist the equalizing effect of bulk diffusion. Inhomogeneities would therefore be even more relevant for finite diffusion. Second, the presence of some exchange of motors between the cytoskeleton and the cytoplasm may in fact simplify a theoretical description, since the approximation of decoupling Eq. (2) yields excellent results for large enough $\Omega > \Omega_c$ (see Figs. 3 and 7). Third, our analysis hints at a way to regulate the spatial distribution of motors, and therefore their cargos, in the cell, by way of modifying the exchange parameter Ω. It can be controlled in independent ways, via ω_D or ω_A (through the bare biochemical rate or through the motor concentration), or via the length dependence in Ω: regulating the cytoskeleton mesh size, for example by crosslinker proteins, would make it possible to control the length scale of heterogeneities. Values reported in the literature [18,23] show that the values used here (Ω, $K \sim O(1)$) are of a reasonable order of magnitude, and it is therefore tempting to speculate that a moderate regulation of Ω might indeed allow a crossover to be provoked between the various regimes in living cells.

We acknowledge support from ANR-09-BLAN-0395-02 and the Scientific Council of the University of Montpellier 2. We thank C. Leduc for discussions and useful references, and C. M. Romano for useful comments and for carefully reading the manuscript.

[1] S. Ramaswamy, Annu. Rev. Condens. Matter Phys. **1**, 323 (2010); M. C. Marchetti, J. F. Joanny, S. Ramaswamy, T. B. Liverpool, J. Prost, M. Rao, and R. A. Simha, arXiv:1207.2929v1; T. Vicsek, A. Czirok, E. Ben-Jacob, I. Cohen, and O. Shochet, Phys. Rev. Lett. **75**, 1226 (1995).

[2] B. Alberts, A. Johnson, J. Lewis, M. Raff, K. Roberts, and P. Walter, *Molecular Biology of the Cell* (Garland Science, Taylor & Francis Group, New York, 2008), 5th ed.

[3] J. L. Ross, M. Y. Ali, and D. M. Warshaw, Curr. Opin. Cell Biol. **20**, 41 (2008).

[4] J. Howard, *Mechanics of Motor Proteins and the Cytoskeleton* (Sinauer Associates, Inc., Sunderland, 2001).

[5] D. A. Fletcher and R. D. Mullins, Nature (London) **463**, 485 (2010).

[6] D. Cai, D. P. McEwen, J. R. Martens, E. Meyhofer, and K. J. Verhey, PLoS Biol. **7**, e1000216 (2009); J. Yoo, T. Kambara, K. Gonda, and H. Higuchi, Exp. Cell Res. **314**, 3563 (2008); P. Pierobon, S. Achouri, S. Courty, A. R. Dunn, J. A. Spudich, M. Dahan, and G. Capello, Biophys. J. **96**, 4268 (2009).

[7] F. Nédélec, T. Surrey, and A. C. Maggs, Phys. Rev. Lett. **86**, 3192 (2001); P. K. Trong, J. Guck, and R. E. Goldstein, Phys. Rev. Lett. **109**, 028104 (2012).

[8] S. Klumpp and R. Lipowsky, Phys. Rev. Lett. **95**, 268102 (2005); S. Klumpp, T. M. Nieuwenhuizen, and R. Lipowsky, Biophys. J. **88**, 3118 (2005).

[9] P. Greulich and L. Santen, Eur. Phys. J. E: Soft Matter Biol. Phys. **32**, 191 (2010).

[10] J. T. MacDonald, J. H. Gibbs, and A. C. Pipkin, Biopolymers **6**, 1 (1968); B. Derrida, E. Domany, and D. Mukamel, J. Stat. Phys. **69**, 667 (1992); T. Chou, K. Mallick, and R. K. P. Zia, Rep. Prog. Phys. **74**, 116601 (2011).

[11] I. Neri, N. Kern, and A. Parmeggiani, Phys. Rev. Lett. **107**, 068702 (2011).

[12] R. Fowler, *Statistical Mechanics* (Cambridge University Press, Cambridge, England, 1936).

[13] K. Mallick, J. Stat. Mech. (2011) P01024.

[14] T. Chou and D. Lohse, Phys. Rev. Lett. **82**, 3552 (1999).

[15] T. Karzig and F. von Oppen, Phys. Rev. B **81**, 045317 (2010).

[16] A. Schadschneider, Physica (Amsterdam) **285A**, 101 (2000); D. Helbing, Rev. Mod. Phys. **73**, 1067 (2001).

[17] A. Parmeggiani, T. Franosch, and E. Frey, Phys. Rev. Lett. **90**, 086601 (2003); Phys. Rev. E **70**, 046101 (2004).

[18] C. Leduc, K. Padberg-Gehle, V. Varga, D. Helbing, S. Diez, and J. Howard, Proc. Natl. Acad. Sci. U.S.A. **109**, 6100 (2012).

[19] A. Barrat, M. Barthélemy, and A. Vespignani, *Dynamical Processes on Complex Networks* (Cambridge University Press, Cambridge, England, 2008).

[20] See Supplemental Material at http://link.aps.org/supplemental/10.1103/PhysRevLett.110.098102 for the full mean field equations and decoupling at high exchange rates: the simplified mean field equations.

[21] B. Embley, A. Parmeggiani, and N. Kern, Phys. Rev. E **80**, 041128 (2009).

[22] I. Neri, N. Kern, and A. Parmeggiani (to be published).

[23] V. C. Varga, C. Leduc, V. Bormuth, S. Diez, and J. Howard, Cell **138**, 1174 (2009); L. Reese, A. Melbinger, and E. Frey, Biophys. J. **101**, 2190 (2011).

[24] L. B. Shaw, R. K. P. Zia, and K. H. Lee, Phys. Rev. E **68**, 021910 (2003).

[25] S. Muhuri and I. Pagonabarraga, Europhys. Lett. **84**, 58 009 (2008)

[26] S. Sandow, Phys. Rev. E **50**, 2660 (1994).

[27] A. Raguin, A. Parmeggiani, and N. Kern to be published.

[28] H. Hinsch and E. Frey, Phys. Rev. Lett. **97**, 095701 (2006); K. Tsekouras and A. B. Kolomeisky, J. Phys. A **41**, 465001 (2008); M. Ebbinghaus and L. Santen, J. Stat. Mech. (2009) P03030.